

IN-CAT. 05

VIRGINIA TECH

76295 CR

P.32

## SEMI-ANNUAL REPORT

# FACTORS AFFECTING THE STICKING OF INSECTS ON MODIFIED AIRCRAFT WINGS

BY

O. YI, M. R. CHITSAZ-Z, N. S. EISS AND  
J. P. WIGHTMAN

(NASA-CR-180957) FACTORS AFFECTING THE  
STICKING OF INSECTS ON MODIFIED AIRCRAFT  
WINGS Semiannual Report, 15 Jun. - 30 Dec.  
1986 (Virginia Polytechnic Inst. and State  
Univ.) 32 p Avail: NTIS HC A03/MF A01

N87-26037

Unclas  
G3/05 0076295

VIRGINIA POLYTECHNIC INSTITUTE  
AND STATE UNIVERSITY

CHEMISTRY DEPARTMENT  
703-961-5854

MECHANICAL ENGINEERING DEPARTMENT  
703-961-7192

SEMI-ANNUAL REPORT

FACTORS AFFECTING THE STICKING OF INSECTS  
ON MODIFIED AIRCRAFT WINGS

BY

O. YI, M. R. CHITSAZ-Z, N. S. EISS AND J. P. WIGHTMAN

PREPARED FOR

NATIONAL AERONAUTICS AND SPACE ADMINISTRATION

NASA - Langley Research Center

Transonic Aerodynamics Division

Hampton, VA 23665

D. Somers

Grant #NAG-1-300

from

Chemistry Department and Mechanical Engineering Department

Virginia Polytechnic Institute and State University

Blacksburg, VA 24061

February, 1987

\*This report covers the period June 15, 1986 to December 30, 1986.

## I. Introduction

A past study by Siochi (1) showed that the surface energy of a polymer coating has an important effect on the sticking of insects to the surface. However, mechanical properties of polymer coatings such as elasticity may also be important. A further study is suggested using polymer coatings of known surface energy and modulus so that a better understanding of the mechanism of the sticking of insects to surfaces can be achieved. As the first step for the study, surface analysis and road tests were performed using elastomers having different energies and different moduli. The number of surface insects sticking on each elastomer was counted and compared from sample to sample and with a control (aluminum). An average height moment was also calculated and comparisons made between samples.

## II. Background

When a drop of liquid is placed on a solid, it will either wet the solid or remain as a drop. The liquid drop may have a definite angle between the liquid and solid phase (2) as shown in Figure 1. The angle ( $\theta$ ) is the contact angle and is defined as the angle through the liquid between a line drawn tangent to the liquid/solid contact point and the solid surface. It is important to notice that a non-uniform surface, due to surface roughness or surface contamination, can change the contact angle.

At equilibrium, interfacial surface tensions and the contact angle  $\theta$  are related by the expression (3)

$$\gamma_{sv} - \gamma_{sl} - \gamma_{lv} \cos\theta = 0 \quad [1]$$

where  $\gamma_{sv}$ ,  $\gamma_{sl}$ , and  $\gamma_{lv}$  are the interfacial surface tensions of the solid-vapor, solid-liquid, and liquid-vapor interfaces, respectively. It is assumed that the difference between  $\gamma_{sv}$  and  $\gamma_s$  (surface tension of solid not in

equilibrium with vapor) is negligible. This equation can be re-written (3) as

$$W_{sl} = \gamma_{lv} (1 + \cos \theta) \quad [2]$$

where  $W_{sl}$  is defined as the work of adhesion or the work required to separate the solid and liquid phases. As the contact angle decreases, the work of adhesion will increase. The liquid is said to spread at a contact angle of  $0^\circ$  corresponding to the maximum work of adhesion.

Zisman and co-workers observed that  $\cos \theta$  (advancing angle) is usually a monotonic function of liquid surface tension for a homologous series of liquids (3). A plot of  $\cos \theta$  versus liquid surface tension ( $\gamma_{lv}$ ) for various series of liquids on a given solid surface is extrapolated to zero  $\theta$  corresponding to a certain liquid surface tension. Zisman called this extrapolated value of liquid surface tension, the critical surface tension of the solid,  $\gamma_c$ .

The scanning electron microscope (SEM) is widely used to examine surface topography (3), and resolution to a few nanometers is possible, depending on the nature of the sample and the type of microscope. A simplified block diagram of an SEM is provided in Figure 2 (4).

X-ray photoelectron spectroscopy (XPS) or electron spectroscopy for chemical analysis (ESCA) was originated by Professor Siegbahn at Uppsala University in Sweden (4). It is a sensitive and quantitative surface technique which can give elemental identification and chemical bond information of solid surfaces. The simplified process for the ESCA technique (5) is shown in Figure 3, and this process can be described (4,5) by the following energy-balance equation:

$$h\nu = E_k + E_b + \phi_s \quad [3]$$

where  $h\nu$  is the energy of the incident x-ray beam,  $E_k$  is the kinetic energy of the photoelectron,  $E_b$  is the binding energy of the photoelectron, and  $\phi_s$  is

the sample work function. Thus, the incident x-ray beam with known energy photoelectrons, whose kinetic energy is measured. Since the  $E_b$  is a fundamental property of an element, the elements present on the sample surface can be identified from the ESCA spectra. Further ESCA can detect a small change in  $E_b$  which is affected by the chemical environment. In other words, chemical shifts due to the differences in the chemical bonding in atoms within molecules may be detected by ESCA.

The atomic concentration or atomic fraction (AF) can be calculated by the equations

$$AF = X / \Sigma X \quad [4]$$

$$X = (A/SW) / (E_k * MFP * X\text{-sec}) \quad [5]$$

where A and SW are the area under the photopeak and sweep number, respectively, obtained from the ESCA spectra; MFP and X-sec are the mean free path and photoelectron cross section, respectively.

A material is called elastic when the deformation produced in the body is completely recovered after the applied force is removed. The modulus of elasticity in tension, or Young's modulus (E) is (2)

$$E = \sigma / \tau \quad [6]$$

where  $\sigma$  is the tensile stress which is the normal force acting per unit area of a plane, and  $\tau$  is the tensile strain or deformation which is the elongation per unit length (2). A better elastomer will have a higher deformation or a smaller modulus.

### III. Experimental

#### **1. Materials Used**

Eight different types of elastomers were studied: five fluorocarbon elastomers (FCE) with different fluorine compositions and physical properties,

Neoprene, Viton<sup>R</sup>, and polyurethane of two different thicknesses. FCE's (6 x 6 x 1/16 in.) were received from 3M; two samples (A & B) contain 69% fluorine, and the other samples (C, D & E) contain 66% fluorine. Neoprene and Viton<sup>R</sup> (6 x 6 x 1/16 in.) were received from duPont. Polyurethane films were pressed from estanes (Goodrich) with 31% hard segments in 6 x 6 in. molds with thicknesses of 1/32 in. and 1/16 in. at two different temperatures of 150°C and 190°C. All elastomer sheets were stored in the dessicator over Drierite.

## 2. Surface Analysis

There was the definite possibility of contamination on the elastomer surfaces, especially grease from mold release agents or during pressing and handling. The elastomers were washed in a solution of Tide<sup>R</sup> and deionized water, and subsequently rinsed with deionized water at least 10 times. The washed elastomers were dried over-night in a vacuum oven at room temperature. The unwashed and washed elastomer surfaces were analyzed by contact angle measurements, SEM and ESCA.

The contact angles of the washed and unwashed FCE and polyurethane samples were measured with (deionized) water using an NRL contact angle goniometer. Since no information on roughness or homogeneity of any sample surfaces were given, a large number of measurements was necessary to reduce errors. First, 2 µl was added to the 2 µl water placed previously and the contact angle was measured. This procedure was repeated two times more so that the total volume of water on the sample surface was 8 µl. contact angles were measured at a minimum of three different locations on the sample surface, and the average contact angle was calculated.

The critical surface tensions for all the sample elastomers were determined from contact angle measurements. At least eight - 1 x 1 in. disks were cut from each elastomer sheet as well as an aluminum sheet, and prepared

as described above. The dried samples were stored in sample bottles to minimize contamination. The contact angles were measured as before using an NRL contact angle goniometer with water/ethanol solutions. Pure ethanol and deionized water were mixed at six different water to ethanol volume ratios: 100/0, 90/10, 70/30, 50/50, 60/40, 70/30, and 80/20. The critical surface tension ( $\gamma_c$ ) was obtained from the plot of  $\cos \theta$  versus liquid surface tension of water/ethanol solutions.

A disk was punched from each washed and unwashed samples, and sputter coated with gold by an SPI sputter coater for 45 seconds at 35mA. SEM photomicrographs of both washed and unwashed samples were taken using a JEOL 35C SEM at two different magnifications (x200 and x360).

The sample surfaces were analyzed quantitatively using ESCA. A 0.9 x 2.0 cm disk was taken from each sample, and ESCA spectra were obtained at 90° take-off angle using a Kratos XSAM 800 x-ray photoelectron spectrometer with a Mg  $K_{\alpha}$  x-ray source. Washed and unwashed samples of polyurethane and FCE (A, B & C) were studied. All washed sample surfaces were also analyzed at 20° take-off angle.

### 3. Collecting and Counting Insects

Five-0.75 x 6 in. strips of each elastomer were washed and dried as described above, and adhesively bonded to 1 x 8 in. aluminum strips. To remove any grease from the contact surfaces, the aluminum surfaces were wiped with "Kemkit" wetted with pure acetone and the elastomer surfaces were washed with pure ethanol.

Adhesives received from the LORD Chemical Corporation were used to glue the elastomer strips to the aluminum substrate. Viton<sup>R</sup>, polyurethane and FCE strips were glued to the aluminum strips using Chemlok<sup>R</sup> (cyanoacrylate adhesive), and pressed between two aluminum strips for at least 30 seconds.

Neoprene strips were glued using Chemlok 234B (mixture of xylene, trichlorethylene, and carbon black), and pressed between two aluminum strips. The ends were cramped and placed in the hot oven at 180°F for two hours.

The sample strips prepared as above and five aluminum strips were mounted on either aluminum or PVC half cylinders (40 in. long and 4 in. to 5 in. outside diameter) as shown in the Figure 4. These cylinders were then mounted on the top of a car, and driven around a loop on Route 618 in Gloucester County, Virginia between 1905 and 2020 hrs on September 7, 1986 to collect insects. The insects collected on all the samples were counted with the naked eye. The stagnation line is the line which divides the sample surface into two, so that the wings of insects on each side of the line point in opposite directions. The distance from the stagnation line to the insects collected on the surfaces was measured with a ruler, and heights of the insects above the surface were measured with a Wild-Heerbrugg M-420 microscope. To measure height, the microscope was focused on the surface of the sample. The number on the focusing dial was recorded, and the second number was taken after the microscope was focused on the uppermost part of the insect. The difference between these two numbers was taken as the height of an insect. The average height moment (HM) was calculated as

$$HM = \cdot \sum (\text{Height} * \text{Distance}) / \text{Total No. of Bugs} \quad [7]$$

#### 4. Modulus of Elasticity

Dog-bone specimens were cut from the elastomer samples, and neck lengths and thicknesses were measured. The dog-bones were stretched in an INSTRON at a cross-head speed of 10.0 mm/min until a plot of load (kg) versus elongation (mm) was achieved. A modulus of elasticity (E) for a given sample was calculated from a plot obtained on the INSTRON using the equation

$$E = (\text{slope of the plot} * g * \text{length of neck}) / (\text{area} * C_c) \quad [8]$$



The elongation obtained from the slope of the plot is corrected to the actual elongation using a correction factor - crosshead speed divided by chart speed. The area in the equation [8] is calculated as the product of thickness and width of the neck of the dog-bone;  $g$  is the acceleration of gravity,  $C_c$  is a conversion factor ( $1 \text{ kg m/s}^2/\text{N}$ , or  $32.174 \text{ lb}_m \text{ ft/s}^2/\text{lb}_f$ ).

#### IV. Results and Discussion

The contact angle measurements and ESCA results of washed and unwashed samples are listed in Tables I and II, respectively. The contact angles for unwashed FCE samples are much lower than for washed ones. A lower angle resulted for the polyurethane after washing.

SEM photomicrographs are provided in Figure 5. SEM photomicrographs of the unwashed samples show non-homogeneous surfaces with large numbers of holes or irregular patterns. In contrast, the photomicrographs of washed samples show homogeneous and smooth surfaces with small number of holes or irregular patterns. Thus, washing and rinsing process have removed the non-homogeneous top layer (probably contaminants) of the unwashed sample, and left an apparently clean surface. So the lower contact angles of the unwashed surfaces are caused by a covering layer on the surface. SEM photomicrographs of the polyurethane sample show similar changes as the FCE samples, but the changes are very small. However, the average contact angle of washed polyurethane is lower than for the unwashed one. No clear cause can be concluded from the SEM photomicrographs.

Comparison of ESCA results lead to a clearer understanding of the observed changes in the contact angles due to washing. As shown in Table II, elements are present on the unwashed samples which are not present on the washed samples. Therefore, it can be concluded that these elements formed the

non-homogeneous top layer shown in the SEM photomicrographs but which is removed by washing.

The reason for changes in the contact angles of washed samples can be explained by comparison of the fluorine composition obtained from ESCA spectra. The fluorine composition on a polymer surface has an important effect on the contact angle; the surface with a higher fluorine composition has a lower surface energy and hence a higher contact angle results. The calculated atomic fraction of fluorine on the washed FCE surfaces are higher than on unwashed ones, so that higher contact angles resulted for the washed surfaces. The polyurethane sample shows the opposite result from FCE samples; a very small amount of fluorine (0.7%) has been removed from the surface after washing, but this is not enough information to explain why the smaller contact angle resulted after washing.

Contact angle measurements using water/ethanol solutions with different volume ratios, for sample elastomers and aluminum are summarized in Table III. Large differences are observed between FCE's, neoprene, Vitron<sup>R</sup>, polyurethane, and aluminum for a high water concentration. However, at ethanol concentrations of 70% or higher, similar values of contact angle were obtained for all samples. These measurements cause the extrapolated critical surface tension for all samples shown in Figure 6 and Table IV, to be unexpectedly about 25 dynes/cm, which is close to the surface tension of pure ethanol. Although no definite conclusion is drawn at the present time, one of the possibilities to account for this result is that ethanol preferentially adsorbs on the low energy polymer surfaces and invalidates the use of ethanol/water solutions to measure  $\gamma_c$ .

The calculated elemental atomic fractions are listed in Tables V and VI for two different take-off angles. In general, the atomic composition for all

the samples changes as the take-off angle changes from 20° to 90°. Bulk fluorine concentrations of FCE-A and FCE-B were reported to be the same (69%) while FCE-C, FCE-D and FCE-E were reported to be somewhat lower (66%). However, the surface fluorine concentrations of FCE's calculated from ESCA spectra do not agree with the bulk composition. Differences in chemical composition in the bulk and at the surface of a polymer are well known.

Calculated values of the elastic moduli for the different polymers are given in Table VII. Modulus is a physical property of a material so that it is only dependent on the material itself. Even though the two polyurethane samples are similar chemically, they are two different materials since the films were pressed at two different temperatures. Thus different moduli resulted for these samples.

The total number of insects and calculated average height moments are listed in Table VIII. The results are also plotted in Figures 7 and 8 as a function of modulus. The total number of insects collected on the control (aluminum) samples was much higher than any of the elastomer samples. However, no correlation between average height moment or total number of insects and modulus was obtained. This may be caused either by the technique used to collect insects, or limited sampling, that is, not enough samples for each elastomer. The major problems with the present collection technique are no control or measure of the insect flux and the initial number of impacts.

Since the technique of collecting insects is limited to summer time, and with the difficulty of controlling the number of impacts, the development of a new impact device has been started. It is basically an air-gun which consists of a 1 in. pipe, a T connector, and a nozzle, arranged as shown in the simplified diagram in Figure 9. Compressed air is passed through a nozzle, and the high velocity exit of air from the nozzle creates a suction behind the

nozzle that induces a large inflow of air through the feed chute. This large volume of air is accelerated as it flows past the nozzle creating a high velocity flow of air in the downstream section of the pipe. Any small object, such as an insect, that is placed in the feed chute will be sucked into the pipe, accelerated in the pipe, and ejected from the end of the pipe at high velocity. Initial tests using polyethylene particles indicate that such small objects are ejected at high velocity, although the exact velocity has to be determined.

#### V. Summary

Changes in the energy of polymer surfaces due to washing were detected by contact angle measurements and SEM photomicrographs. The causes of these surface energy changes were explained partially by results obtained from ESCA analysis.

A significant difference between the total number of insects sticking on any elastomer sample and on the aluminum control sample was observed. However, no correlation was obtained between the modulus of the elastomer and the total number of insects sticking or the height moment for a given sample. There may have been large experimental errors introduced during the road test caused by a variable insect flux. A new insect impacting technique is being developed to improve the reproducibility.

#### VI. Future Work

The following recommendations for future work are listed:

1. Another set of contact angle measurements with other liquids - possibly the Zisman series.
2. Determine the exit velocity of polyethylene particles from the "Air-Gun" using strobes, small size particles, and a camera.
3. Use of model particles and/or insects in the Air-Gun.

**VII. REFERENCES**

1. Siochi, A **Fundamental Study of the Sticking of Insect Residues to Aircraft Wings**, M. S. Thesis, VPI&SU, Blacksburg, 1985.
2. Jastrzebski, J. D. **The Nature and Properties of Engineering Materials**, John Wiley & Sons, New York (1977).
3. Adamson, A. W. **Physical Chemistry of Surfaces**, John Wiley & Sons, New York, (1982).
4. Kane, P. F. and G. B. Larrabee Ed., **Characterization of Solid Surfaces**, Plenum Press, New York (1974).
5. Hercules, D. M. and S. H. Hercules, **Analytical Chemistry of Surfaces: Part II. Electron Spectroscopy**, J. Chemical Education, 61, 483, 1984.
6. J. R. Dann, **Forces Involved in the Adhesive Process: 1. Critical Surface Tensions of Polymeric Solids as Determined with Polar Liquids**, J. Colloid Interface Science, 32, 302, 1970.

TABLE I. CONTACT ANGLES OF WASHED AND UNWASHED SAMPLES

	A	B	C	D	E	PU
UNWASHED	76	76	78	77	78	81
WASHED	95	96	96	91	93	71

Note: A-E are the FCE samples and PU is the polyurethane sample.

TABLE II. ESCA ATOMIC COMPOSITION (%) AND RATIOS OF WASHED  
AND UNWASHED ELASTOMER SAMPLES

Sample	Photopeak						
	C 1s	O 1s	F 1s	Si 2p	N 1s	Ca 2p	S 2p
UNWASHED FCE-A	78.	8.5	8.8	2.8	1.5	0.6	0.2
WASHED FCE-A	63.	3.2	33.	0.5	---	---	---
UNWASHED FCE-B	72.	9.0	14.	2.7	1.3	0.5	---
WASHED FCE-B	64.	6.7	28.	1.9	---	---	---
UNWASHED FCE-C	73.	9.1	12.	3.4	1.6	0.4	---
WASHED FCE-C	60.	4.0	36.	0.2	0.2	---	---
UNWASHED PU	82.	13.	0.7	1.7	0.8	1.5	---
WASHED PU	81.	16.	---	0.4	2.4	---	---

	Ratio					
	O/C	F/C	Si/C	N/C	Ca/C	S/Ca
UNWASHED FCE-A	0.11	0.11	0.036	0.019	0.008	0.003
WASHED FCE-A	0.051	0.52	0.008	-	-	-
UNWASHED FCE-B	0.12	0.19	0.038	0.018	0.007	-
WASHED FCE-B	0.10	0.44	0.030	-	-	-
UNWASHED FCE-C	0.12	0.16	0.046	0.022	0.005	-
WASHED FCE-C	0.067	0.60	0.003	0.003	-	-
UNWASHED PU	0.16	0.009	0.021	0.010	0.018	-
WASHED PU	0.20	-	0.005	0.030	-	-

TABLE IIIa. CONTACT ANGLE MEASUREMENTS WITH WATER/ETHANOL SOLUTIONS

Sample	Water/Ethanol (v/v)						
	100/0	90/10	70/30	50/50	40/60	30/70	80/20
FCE - A	92	85	66	50	48	40	25
FCE - B	94	84	70	53	46	39	28
FCE - C	93	78	64	51	48	36	---
FCE - D	96	84	65	47	46	34	23
FCE - E	96	84	67	50	38	31	---
PU	70	60	48	28	23	---	---
NEOPRENE	102	93	75	61	57	39	44
VITON	103	95	76	62	55	49	39

TABLE IIIb. SURFACE TENSION OF WATER/ETHANOL SOLUTION (6)

	Water/Ethanol (v/v)						
	100/0	90/10	70/30	50/50	40/60	30/70	80/20
Surface tension (mJ/m <sup>2</sup> )	72.2	51.3	36.1	30.0	28.0	27.2	25.6



TABLE IV. CALCULATED CRITICAL SURFACE TENSION

Sample	Critical Surface Tension (mJ/m <sup>2</sup> )
FCE - A	24.
FCE - B	24.
FCE - C	24.
FCE - D	26.
FCE - E	26.
PU	25.
NEOPRENE	25.
VITON	24.

TABLE V. ESCA ATOMIC COMPOSITION (%) AND RATOS DETERMINED ON  
ELASTOMER SAMPLES AT A TAKE-OFF ANGLE OF 20°

Sample	Photopeak						
	C 1s	O 1s	F 1s	Si 2p	N 1s	Cl 2p	Pb 4f
FCE - A	59.	2.9	37.	0.7	---	---	---
FCE - B	55.	5.5	37.	2.4	---	---	---
FCE - C	57.	3.7	38.	0.9	0.1	---	---
FCE - D	53.	3.3	43.	0.7	---	---	---
FCE - E	57.	5.1	36.	1.7	---	---	---
PU	81.	17.	---	0.9	---	---	---
NEOPRENE	58.	20.	---	22.	---	0.6	---
VITON	41.	24.	13.	20.	0.7	---	0.4

Sample	Ratio					
	O/C	F/C	Si/C	N/C	Cl/C	Pb/C
FCE - A	0.049	0.63	0.012	--	--	--
FCE - B	0.10	0.67	0.044	--	--	--
FCE - C	0.065	0.67	0.016	0.002	--	--
FCE - D	0.062	0.81	0.013	--	--	--
FCE - E	0.089	0.63	0.030	--	--	--
PU	0.21	--	0.011	--	--	--
NEOPRENE	0.34	--	0.38	--	0.010	--
VITON	0.58	0.32	0.49	0.017	--	0.010

TABLE VI. ESCA ATOMIC COMPOSITION (%) AND RATIOS DETERMINED ON  
ELASTOMER SAMPLES AT A TAKE-OFF ANGLE OF 90°

<u>Sample</u>	<u>Photopeak</u>						
	<u>C 1s</u>	<u>O 1s</u>	<u>F 1s</u>	<u>Si 2p</u>	<u>N 1s</u>	<u>Cl 2p</u>	<u>Pb 4f</u>
FCE - A	53.	3.2	33.	0.5	---	---	---
FCE - B	64.	6.7	28.	1.9	---	---	---
FCE - C	60.	4.0	36.	0.2	0.2	0.2	---
FCE - D	59.	4.3	36.	0.3	---	---	---
FCE - E	60.	5.4	34.	0.7	---	---	---
PU	81.	16.	---	0.4	2.4	---	---
NEOPRENE	62.	20.	---	18.	---	1.1	---
VITON	46.	23.	12.	18.	0.5	---	1.0
<u>Sample</u>	<u>Ratio</u>						
	<u>O/C</u>	<u>F/C</u>	<u>Si/C</u>	<u>N/C</u>	<u>Cl/C</u>	<u>Pb/C</u>	
FCE - A	0.060	0.62	0.009	--	--	--	
FCE - B	0.10	0.44	0.030	--	--	--	
FCE - C	0.067	0.60	0.003	0.003	0.003	--	
FCE - D	0.073	0.61	0.005	--	--	--	
FCE - E	0.090	0.57	0.012	---	--	--	
PU	0.20	--	0.005	0.030	--	--	
NEOPRENE	0.32	--	0.29	--	0.018	--	
VITON	0.50	0.26	0.39	0.011	--	0.022	

TABLE VII. MODULUS OF ELASTICITY

<u>Sample</u>	<u>Modulus of Elasticity (psi)</u>
FCE - A	312.
FCE - B	499.
FCE - C	157.
FCE - D	361.
FCE - E	499.
PU (1/32")	5057.
PU (1/16")	2615.
NEOPRENE	1130.
VITON	860.
ALUMINUM (2)	$1.02 \times 10^7$

TABLE VIII. TOTAL NUMBER OF IMPACTED INSECTS (N)  
AND MEAN HEIGHT MOMENT (MHM)

Sample	N	MHM (in. x 10)
FCE - A	40	26.
FCE - B	48	30.
FCE - C	40	34.
FCE - D	44	25.
FCE - E	59	24.
PU (1/32")	48	20.
PU (1/16")	41	27.
NEOPRENE	43	37.
VITON	49	31.
ALUMINUM	65	26.

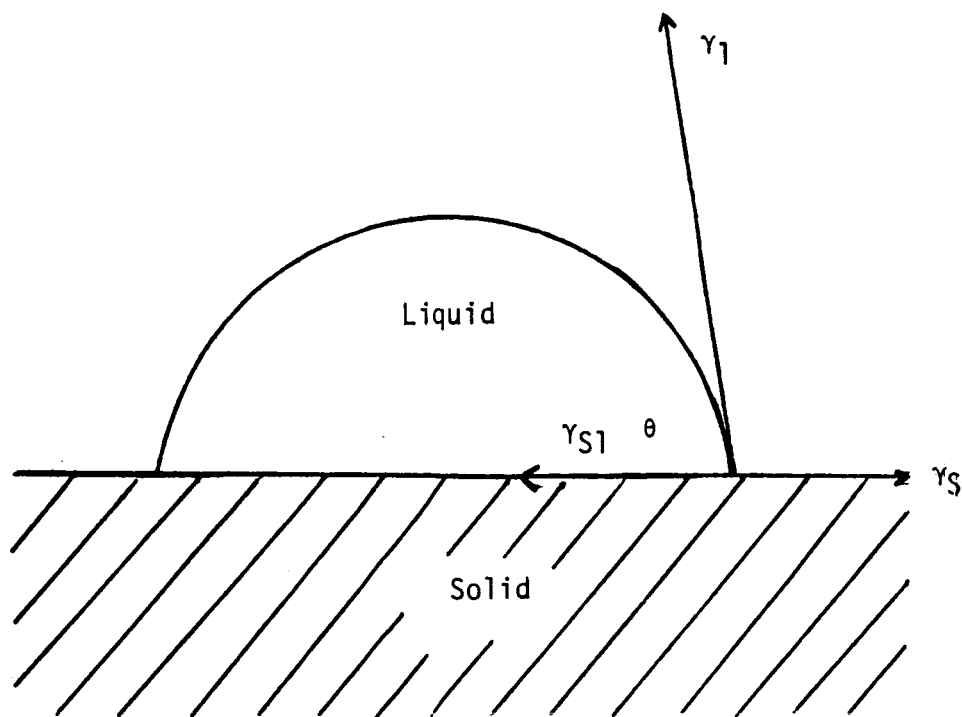


Figure 1. Liquid drop in contact with solid surface  
[ $\theta$  is the contact angle].

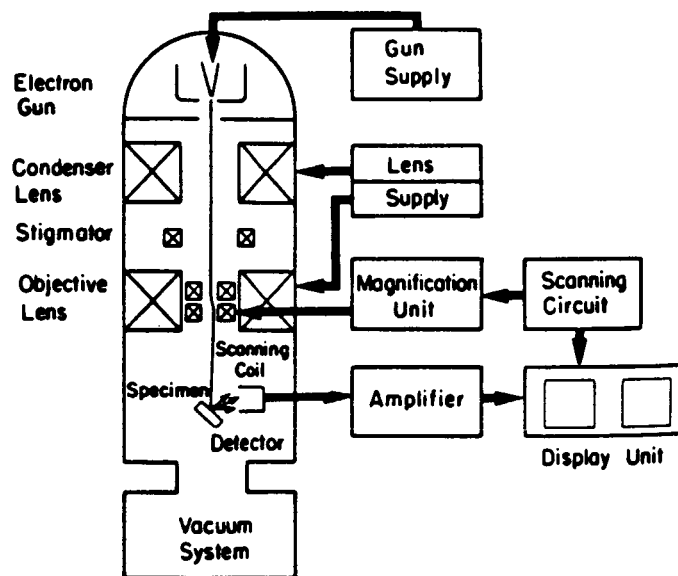


Figure 2. Simplified block diagram of scanning electron microscope.

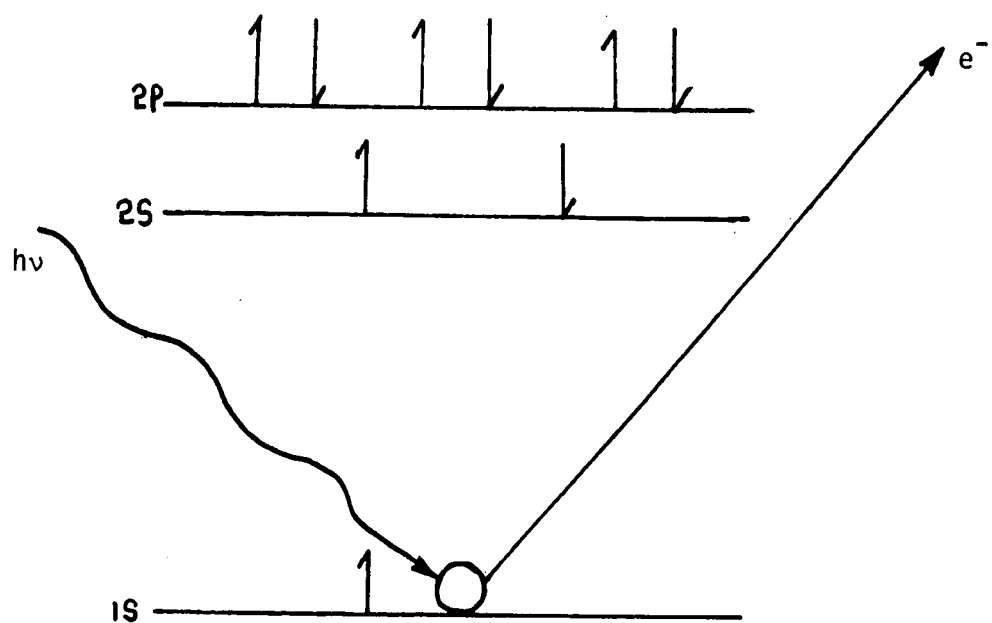


Figure 3. Simplified energy level diagram for ESCA process.



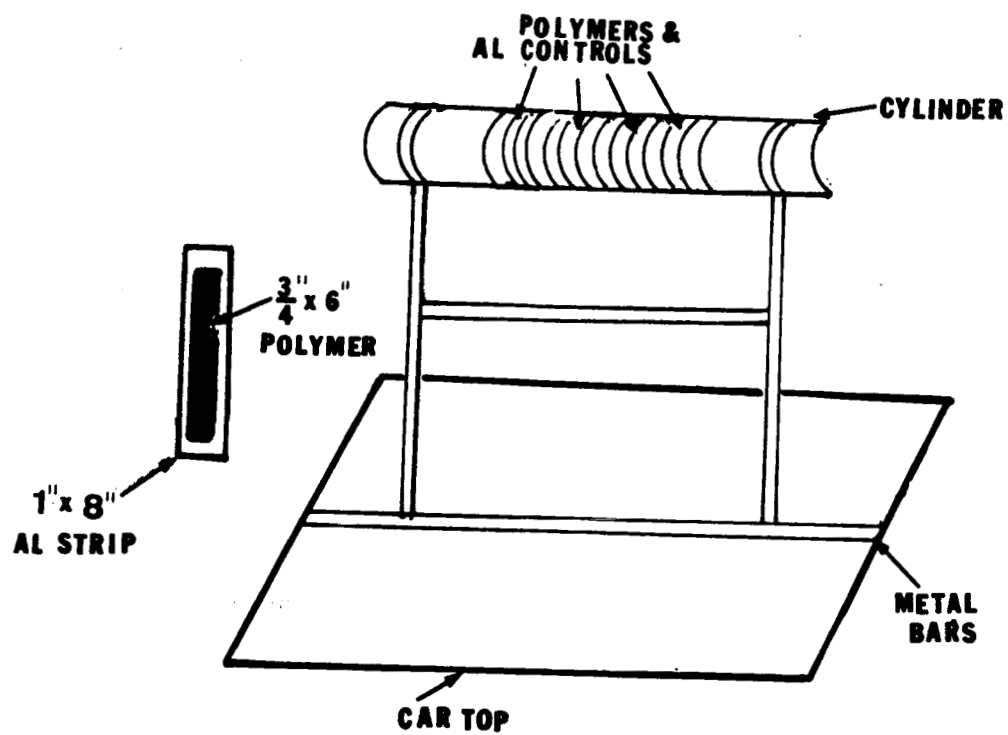
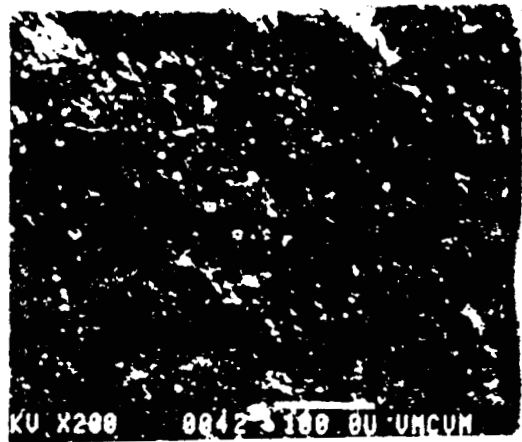


Figure 4. Simplified diagram of an insect collecting device.

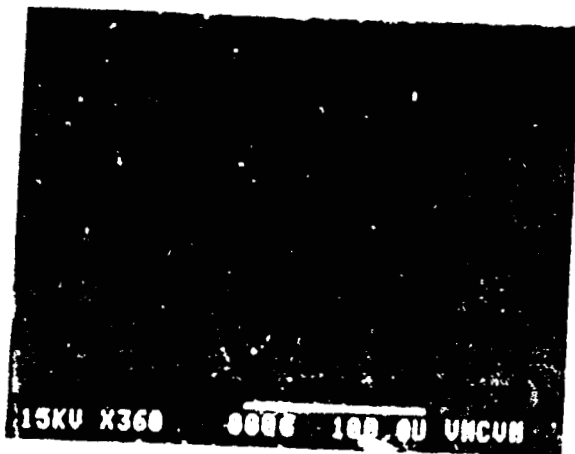
ORIGINAL PAGE IS  
OF POOR QUALITY



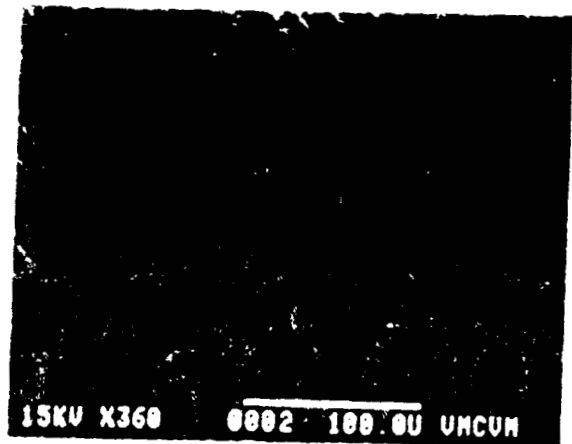
Unwashed Viton



Washed Viton



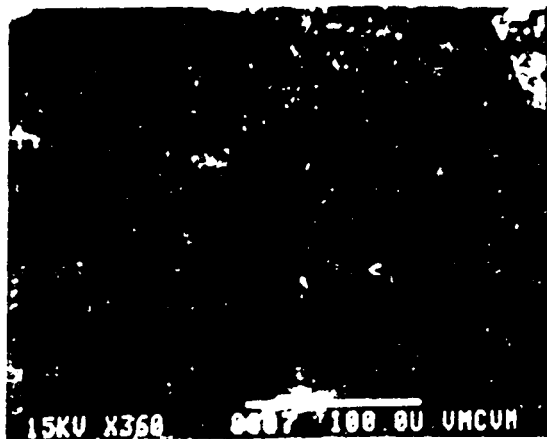
Unwashed Urethane



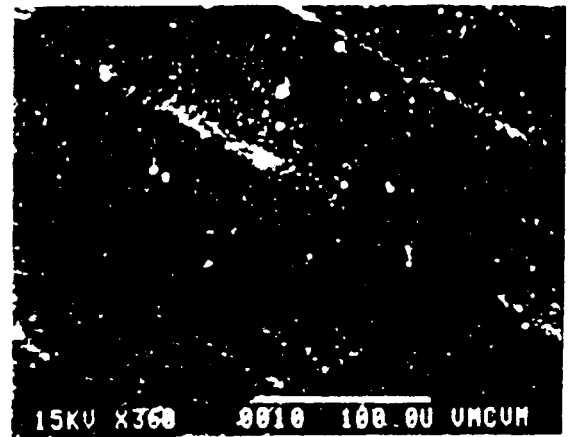
Urethane

Figure 5. SEM photomicrographs of elastomer surfaces.

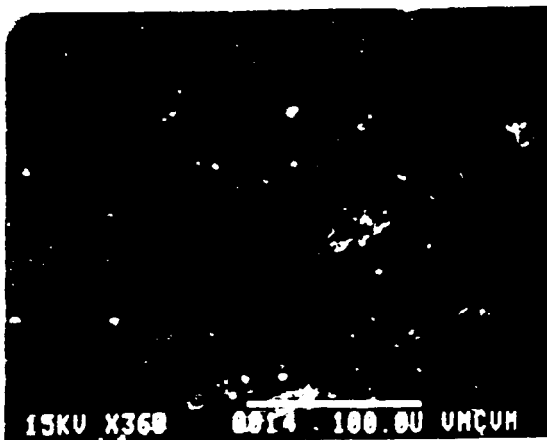
ORIGINAL PAGE IS  
OF POOR QUALITY



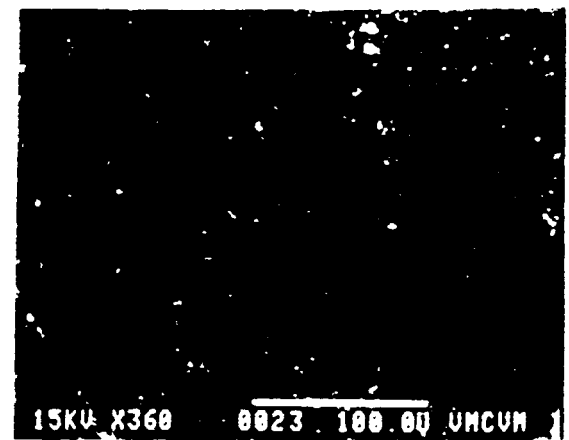
Unwashed FCE-A



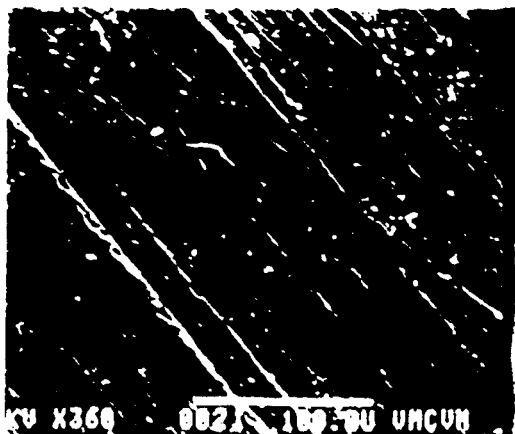
Washed FCE-A



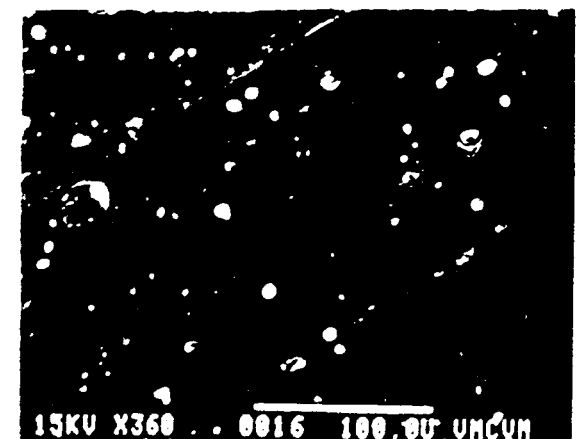
Unwashed FCE-B



Washed FCE-B



Unwashed FCE-C

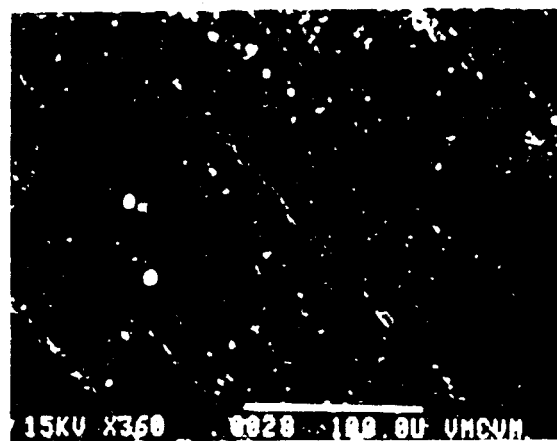


Washed FCE-C

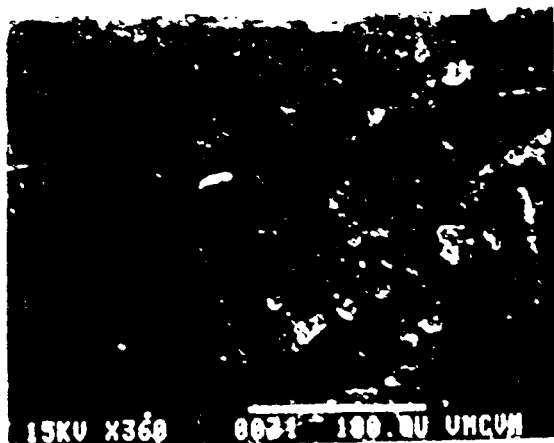
ORIGINAL PAGE IS  
OF POOR QUALITY



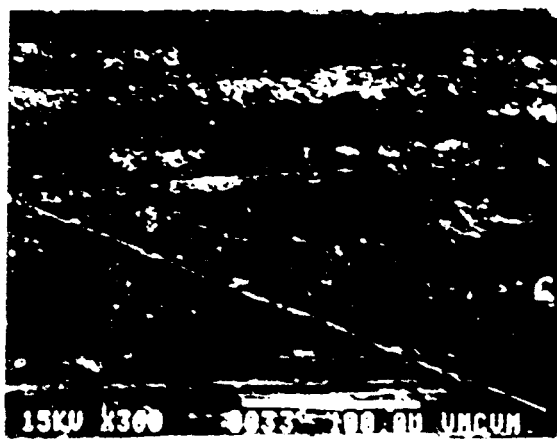
Unwashed FCE-D



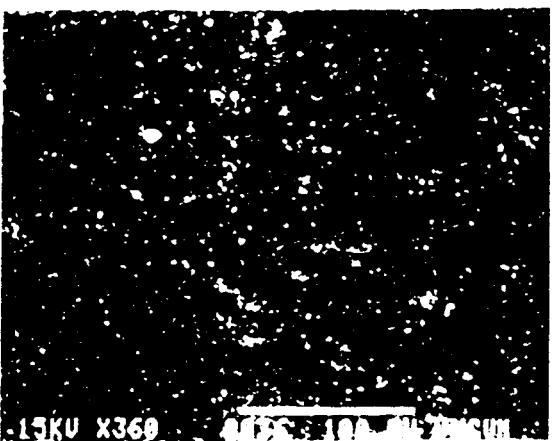
Washed FCE-D



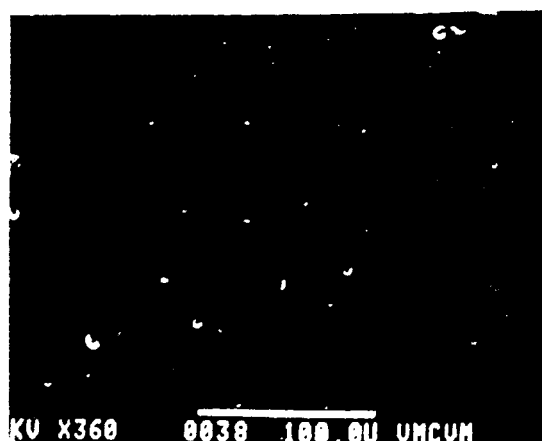
Unwashed FCE-E



Washed FCE-E



Unwashed Neoprene



Washed Neoprene

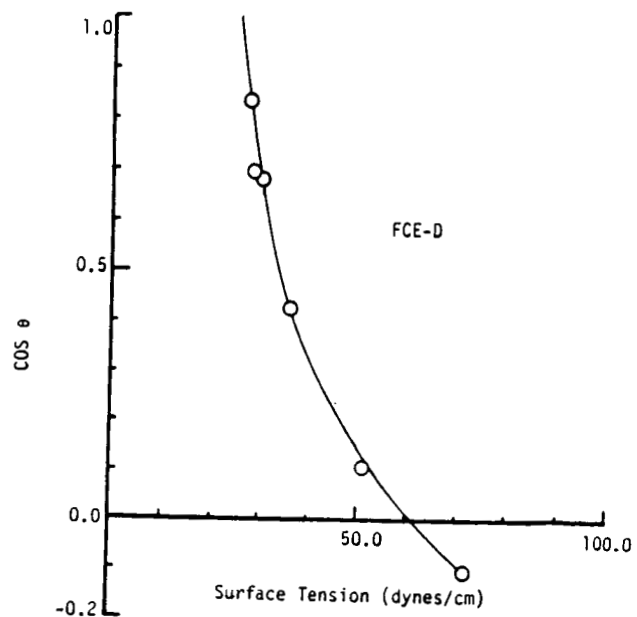
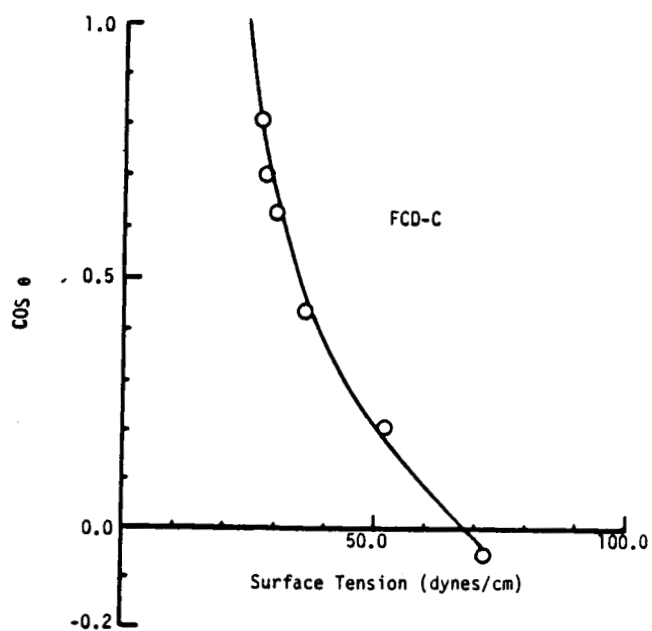
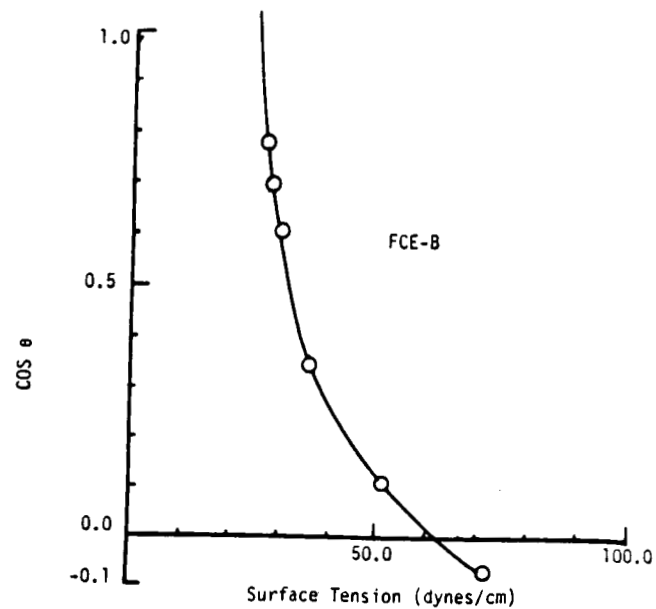
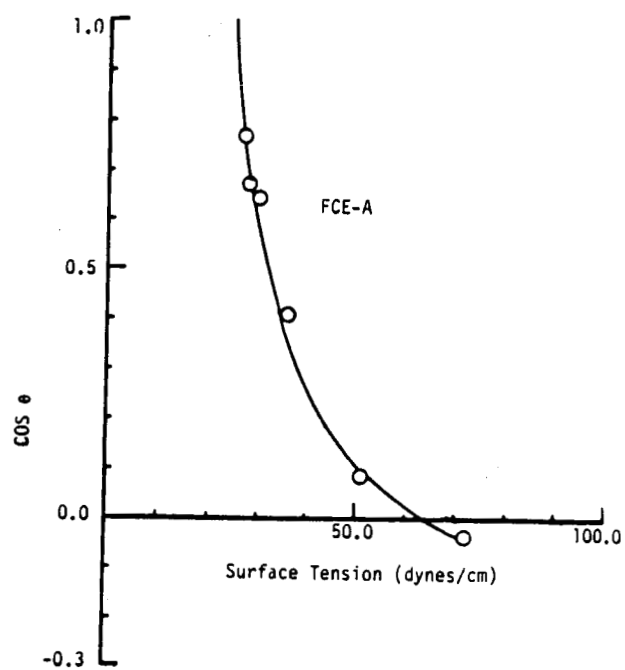
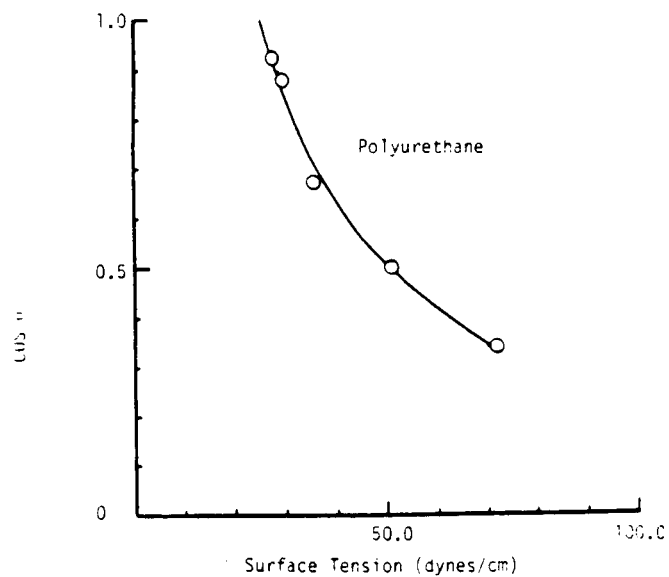
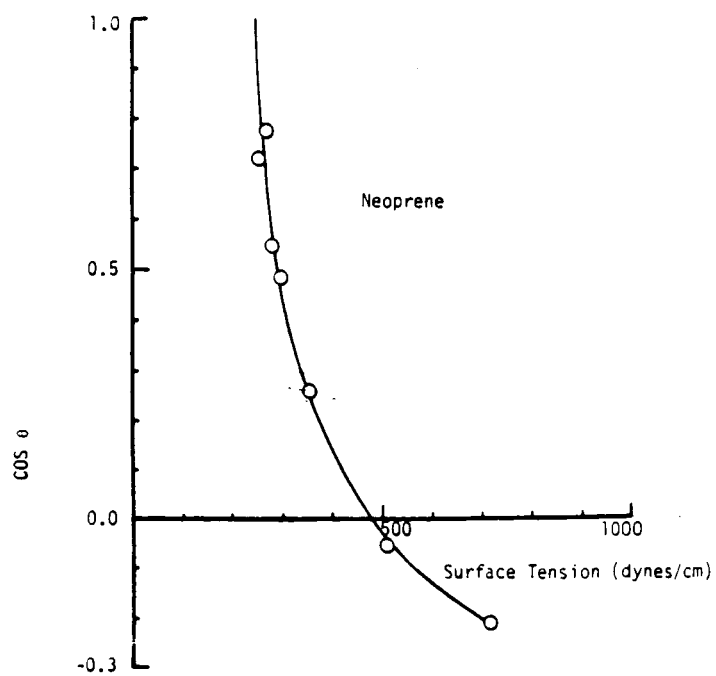
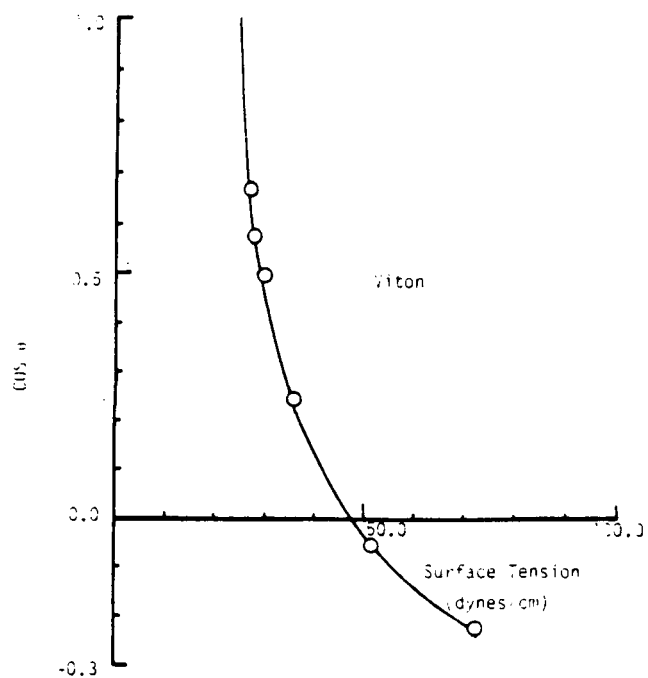
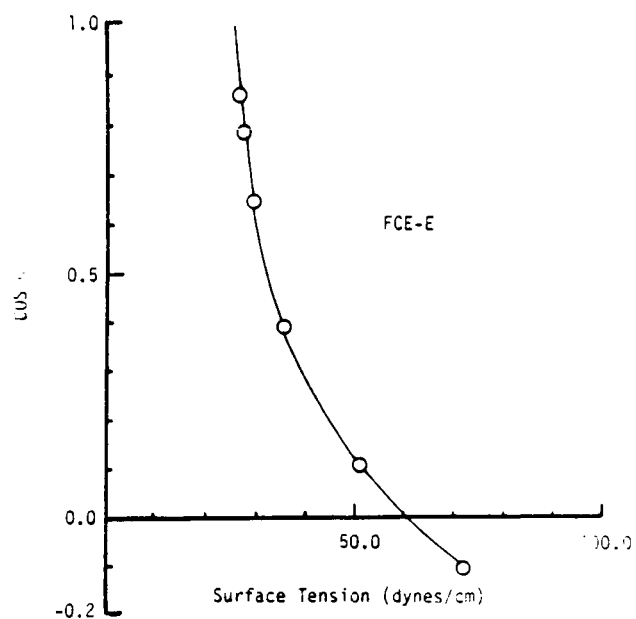


Figure 6.  $\cos \theta$  vs. surface tension of water/ethanol solution

$[\gamma_c$  is at  $\cos \theta = 1]$ .



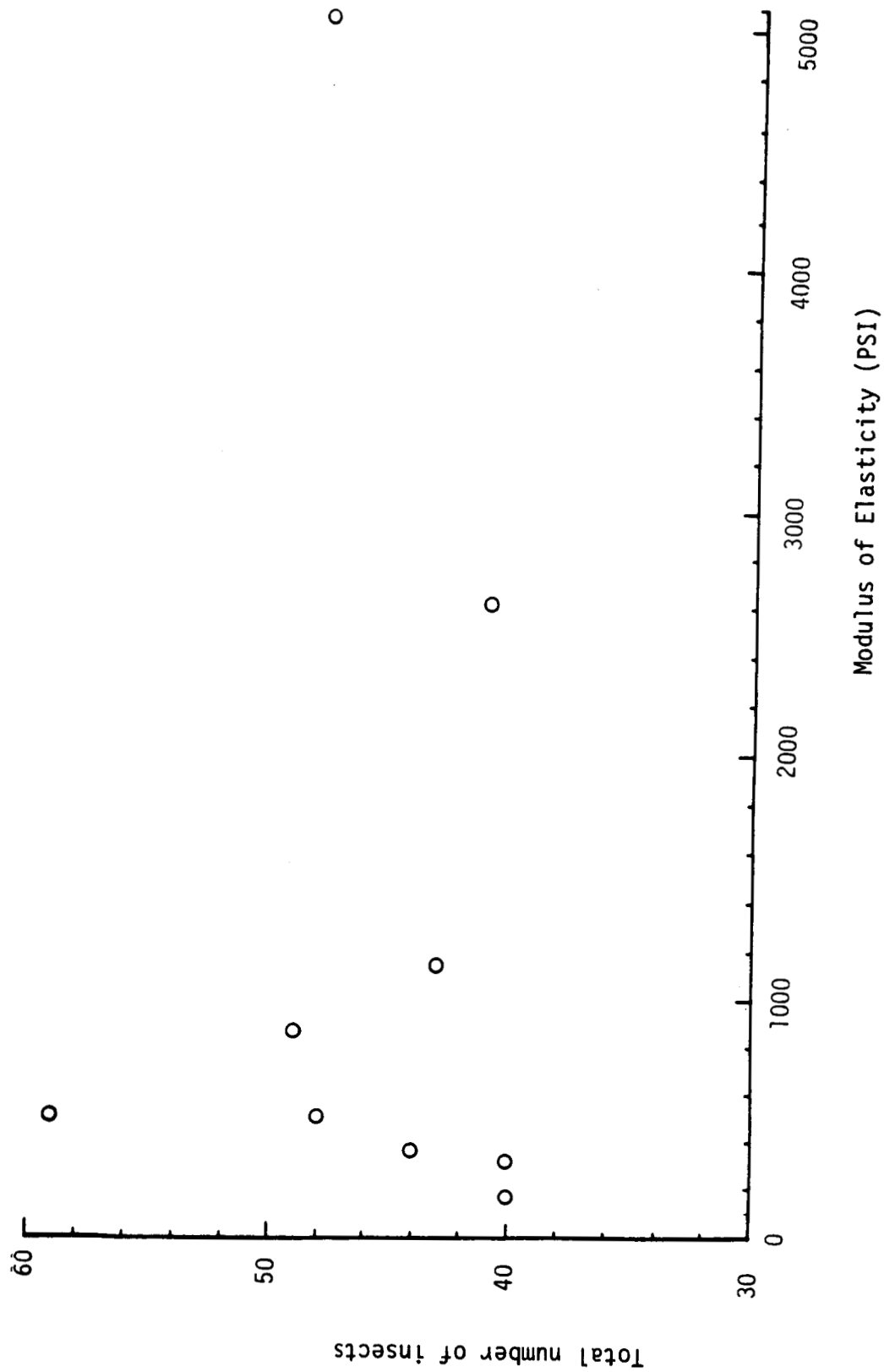


Figure 7. Total number of insects collected vs. modulus of elasticity (psi) for elastomers.

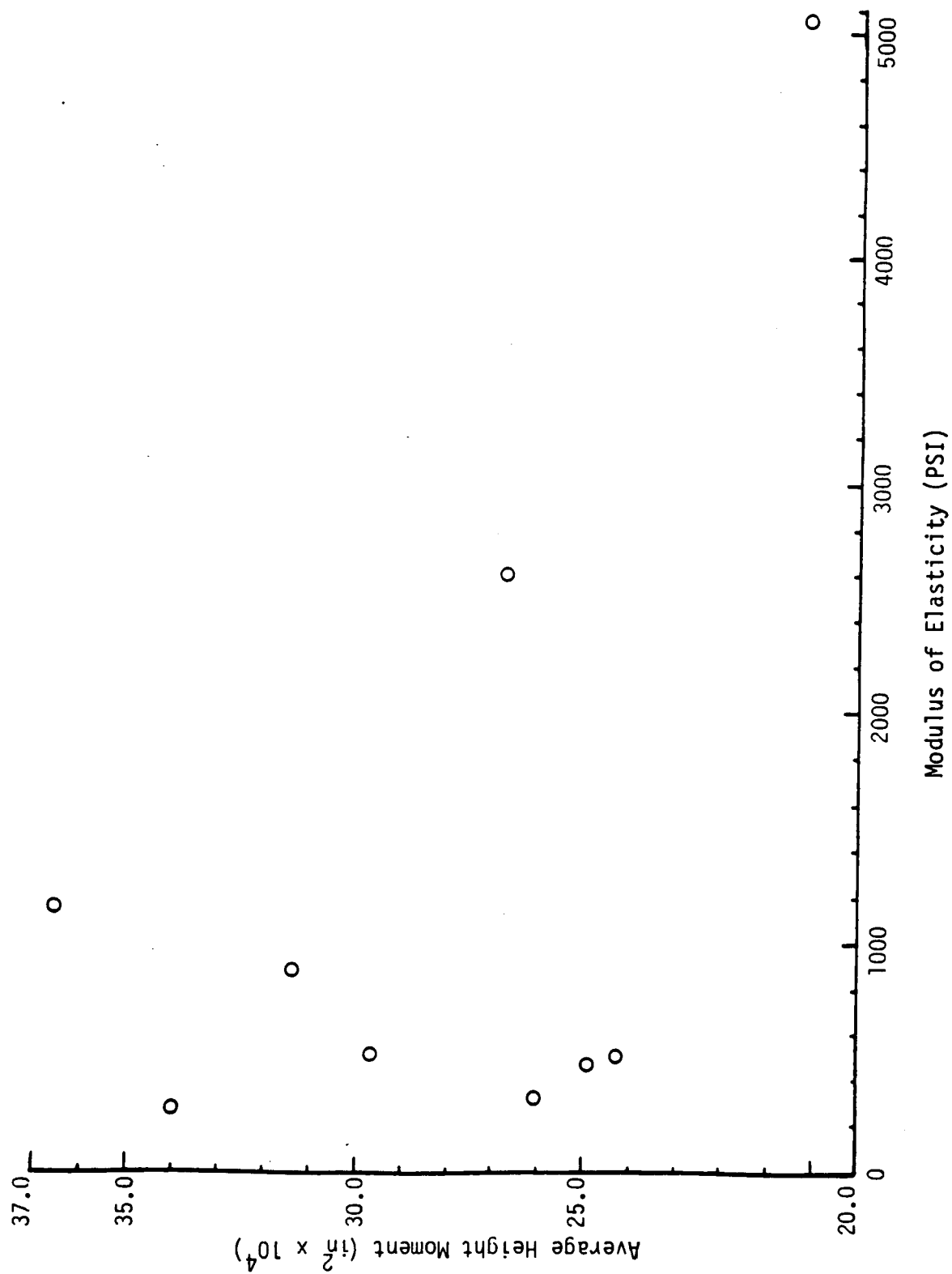


Figure 8. Average height moment vs. modulus of elasticity for elastomers.



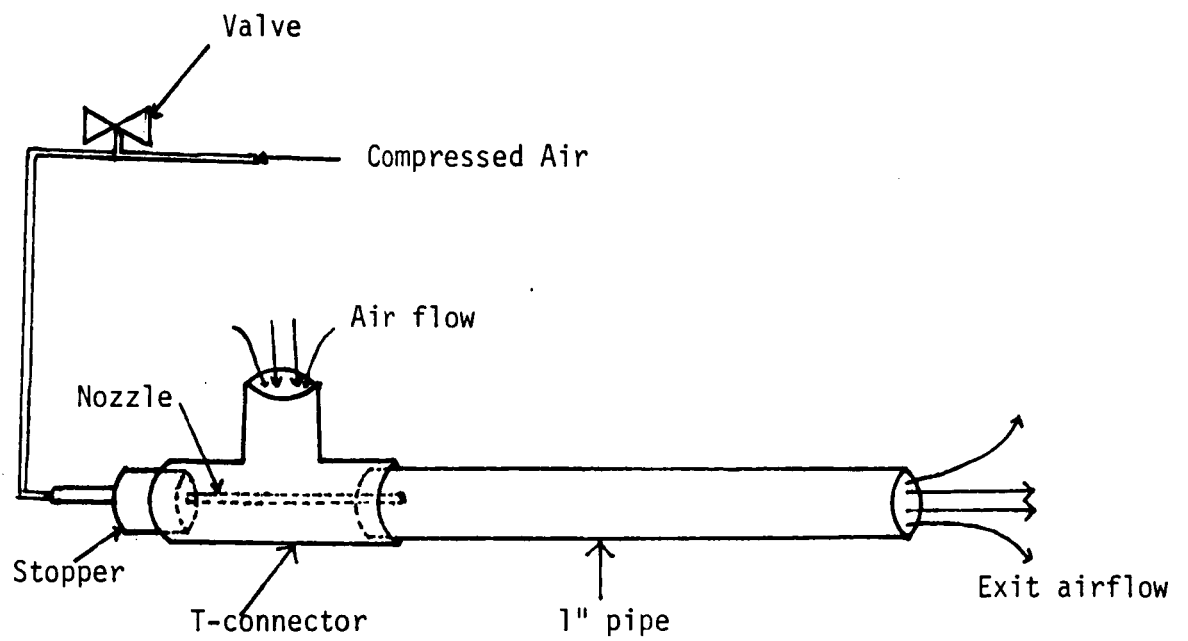


Figure 9. Simplified diagram of "Air-Gun".